ARTICLE

OBC
www.rsc.org/obc

The relative orientation of the lipid and carbohydrate moieties of lipochitooligosaccharides related to nodulation factors depends on lipid chain saturation†‡

Patrick Groves,[a] Stefanie Offermann,[b] Martin Ohsten Rasmussen,[b] F. Javier Cañada,[a] Jean-Jacques Bono,[c] Hugues Driguez,[b] Anne Imberty*[b] and Jesús Jiménez-Barbero*[a]

[a] *Centro de Investigaciones Biológicas, CSIC, Ramiro de Maeztu 9, 28040, Madrid, Spain. E-mail: jjbarbero@cib.csic.es; Fax: 34 915531706; Tel: 34 915346623 ext. 4370*

[b] *Centre de Recherches sur les Macromolecules Vegetales-CNRS (Affiliated with Université Joseph Fourier), BP 53, 38041, Grenoble cedex 9, France. E-mail: Anne.Imberty@cermav.cnrs.fr; Fax: 33 476547203; Tel: 33 476037636*

[c] *UMR 5546-CNRS-Université Paul Sabatier, 24 chemin de Borde Rouge, BP 17 Auzeville, 31326, Castanet-Tolosan, France*

Received 6th January 2005, Accepted 28th February 2005
First published as an Advance Article on the web 9th March 2005

Lipochitooligosaccharides (LCOs) signal the symbiosis of rhizobia with legumes and the formation of nitrogen-fixing root nodules. LCOs **1** and **2** share identical tetrasaccharide scaffolds but different lipid moieties (**1**, LCO-IV(C16:1[9*Z*], SNa) and **2**, LCO-IV(C16:2[2*E*,9*Z*], SNa)). The conformational behaviors of both LCOs were studied by molecular modeling and NMR. Modeling predicts that a small lipid modification would result in a different relative orientation of the lipid and tetrasaccharide moieties. Diffusion ordered spectroscopy reports that both LCOs form small aggregates above 1 mM. Nuclear Overhauser spectroscopy (NOESY) data, collected under monomeric conditions, reveals lipid–carbohydrate contacts only for **1**, in agreement with the modeling data. The distinct molecular structures of **1** and **2** have the potential to contribute to their selective binding by legume proteins.

Introduction

The interaction of nitrogen-fixing rhizobia with legumes is a major topic of interest as this symbiosis promotes soil fertility while lowering the agricultural requirement for chemical fertilizers.[1] Rhizobia produce lipochitooligosaccharides (LCOs, also called Nod factors), which are key symbiotic signals in the molecular dialogue between the prokaryotic and eukaryotic partners leading to successful bacterial invasion into the legume host root.[2–4] LCOs are based on tetra- or penta-saccharide scaffolds formed from linear, β(1–4) linked oligomers of *N*-acetyl glucosamine (GlcNAc) with the terminal non-reducing sugar de-*N*-acetylated and *N*-acylated with a fatty acid. Different rhizobial species produce characteristic Nod factor structures with chemical substitutions on the reducing and non-reducing sugars and variations in the structure of the acyl chain. The range and nature of the Nod factor structures appear to be important for nodulation and rhizobial host specificity.

The physiological relevance of the lipid moiety of LCOs could be related to either a membrane-anchoring role, as supported by Goedhart *et al.*,[5] or a structural requirement for receptor specificity,[3] or a propensity to form micelles. The self-aggregation properties of LCOs are ill-defined but the potential physiological concentrations of LCOs produced by rhizobia, in the confined environment of a curling root, are in the low micromolar range according to Geurts and Bisseling.[6] This concentration might be sufficient to result in LCO aggregates that may have different signaling properties to their monomeric forms. Herein, we describe an investigation of several aspects of LCO structure including the self-aggregating properties of two closely related LCOs, paying special attention to the relative orientation of the lipid and tetrasaccharide moieties of LCOs. We use a combined approach with molecular modeling methods supported by experimental NMR data. The implications of the studied LCO structures on Nod-factor signaling are discussed.

Results and discussion

Fig. 1 shows the structures of the LCOs used in this study. **1** is an active Nod factor analogue whose structure has previously been studied by Gonzalez *et al.*,[7] whereas the second double bond in the lipid moiety of **2** provides a natural Nod factor

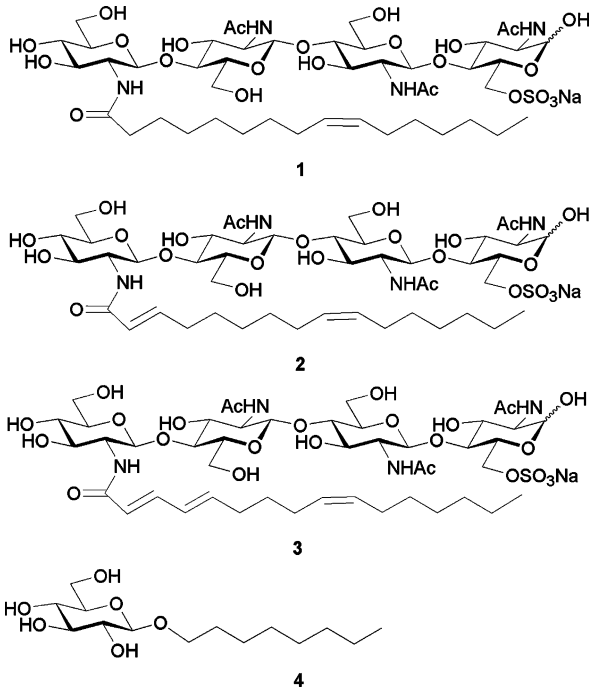

Fig. 1 Structures of LCO **1**, LCO-IV(C16:1[9*Z*], SNa); **2**, LCO-IV(C16:2[2*E*,9*Z*], SNa); **3**, LCO-IV(C16:3[2*E*,4*E*,9*Z*], SNa) and of the detergent β-D-octyl glucopyranoside (**4**).

† Electronic supplementary information (ESI) available: Superimpositions of the characteristic conformations of **1** and **2**. See http://www.rsc.org/suppdata/ob/b5/b500104h/

‡ P. Groves and S. Offermann have contributed equally to this work.

DOI: 10.1039/b500104h

structure. **2** is a synthesized product identical to the main Nod factor produced by *Sinorhizobium meliloti*.[3] **3**, with three double bonds in its lipid moiety, is a native LCO produced in small amounts by *S. meliloti*.[8]

Molecular modeling studies of LCOs

A simulated annealing protocol was applied to obtain information about the conformational behaviors of **1** and **2**. The simulation protocol was applied twice to each molecule and, in each case, 15000 different conformations were produced. Out of these, the 500 final conformations of lowest energy were chosen and analyzed.

Fig. 2 represents the lowest energy conformations of **1** (Fig. 2A, 2B) and **2** (Fig. 2C, 2D). Both views differ in their orientation by a rotation of 90°. The only obvious difference between the conformations derived from **1** or from **2**, respectively, is the relative orientation of the lipid chain (light blue) with respect to the oligosaccharide scaffold. It appears more stretched and tends to align with the oligosaccharide part (colored) for **1** whereas for **2**, the lipid exhibits a more bent behavior and tends to form conformations that are more orthogonal to the tetrasaccharide.

More information about the different behaviors of **1** and **2** can be obtained from a geometrical analysis whose results are partially shown in Fig. 3. The 500 lowest energy conformations have been classified in families depending on their angle α (blue) or torsional angle β (green), respectively, which are shown in the inset diagram of Fig. 3. Both angles are situated in the connection between the oligosaccharide and lipid moieties. These angles were chosen as they most obviously illustrate the structural differences between **1** and **2**, depending on the one additional *cis* double bond of **2**. The diagrams point to a varying distribution of both angles in molecules **1** and **2**: for **1**, the majority of conformations have an angle α of around 108° to 116°, whereas for **2** this angle is significantly larger and the maximum lies between 124° and 130° (Fig. 3A). The spread of the torsional angle β is more diverse and contains three maxima and minima for both molecules with different distributions. The conformations of **1** mainly adopt a angle β torsion of ±90. In contrast, the maxima of **2** have a β angle that is orthogonal, around ±180° (Fig. 3B). Due to stereochemical rules, the different behavior of the angle α between **1** and **2** is not unexpected. However, the different performance of torsional angle β cannot simply be attributed to the additional *cis* double bond in the lipid chain of **2**, but to different interactions between the lipid chain and the sugar chain in **1** *versus* **2**.

The results of the geometrical analysis were used to create superimpositions of the characteristic conformations of **1** and **2**, as shown in Fig. S1 in the supporting information.† The fifty lowest energy conformations out of the mostly occupied range of the angle α have been superimposed using the first sugar ring as the initial point. Generally, Fig. S1 demonstrates the high flexibility of the oligosaccharide of **1**, as well as of **2**, but this seems to be slightly more restricted for the LCO conformations obtained from **1**. Also, the lipid chains (grey) in most conformations of **1** occupy a more limited space as the lipid chains remain close to the oligosaccharide moiety.

Further calculations were performed on a LCO containing three double bonds (**3**).[8] Again, another distinct distribution of the angle α (maximum population around 120°) and the torsional angle β (around ±180° with an additional, less populated geometry around 0°) was observed (data not shown), which supports our theory that small modifications such as a single double bond suffice to change the shape of the whole LCO molecule.

The aggregation state of LCOs measured by DOSY-NMR

Fig. 4 shows the critical micelle concentrations (CMCs) of a number of detergents consisting of lipids linked to mono-, di- and tri-saccharides as a function of the length of the lipid moiety, including β-D-octyl glucopyranoside, **4**. The data in

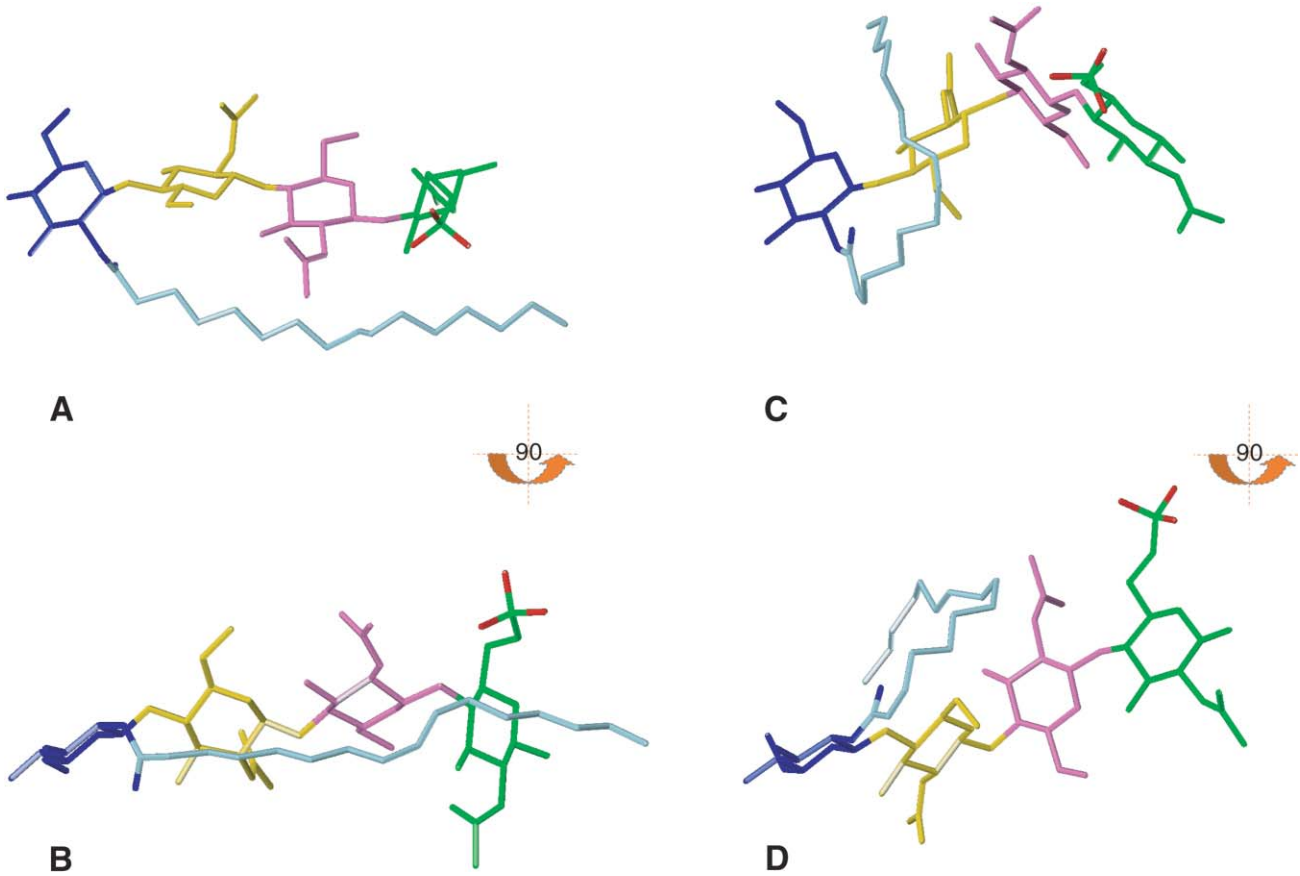

Fig. 2 Lowest energy conformations of **1** (A, B), and **2** (C, D). The two images differ from the lower ones by a 90° rotation. The four residues of the sugar moiety are shown in different colors (blue, yellow, rose, green), the lipid moiety is colored light blue.

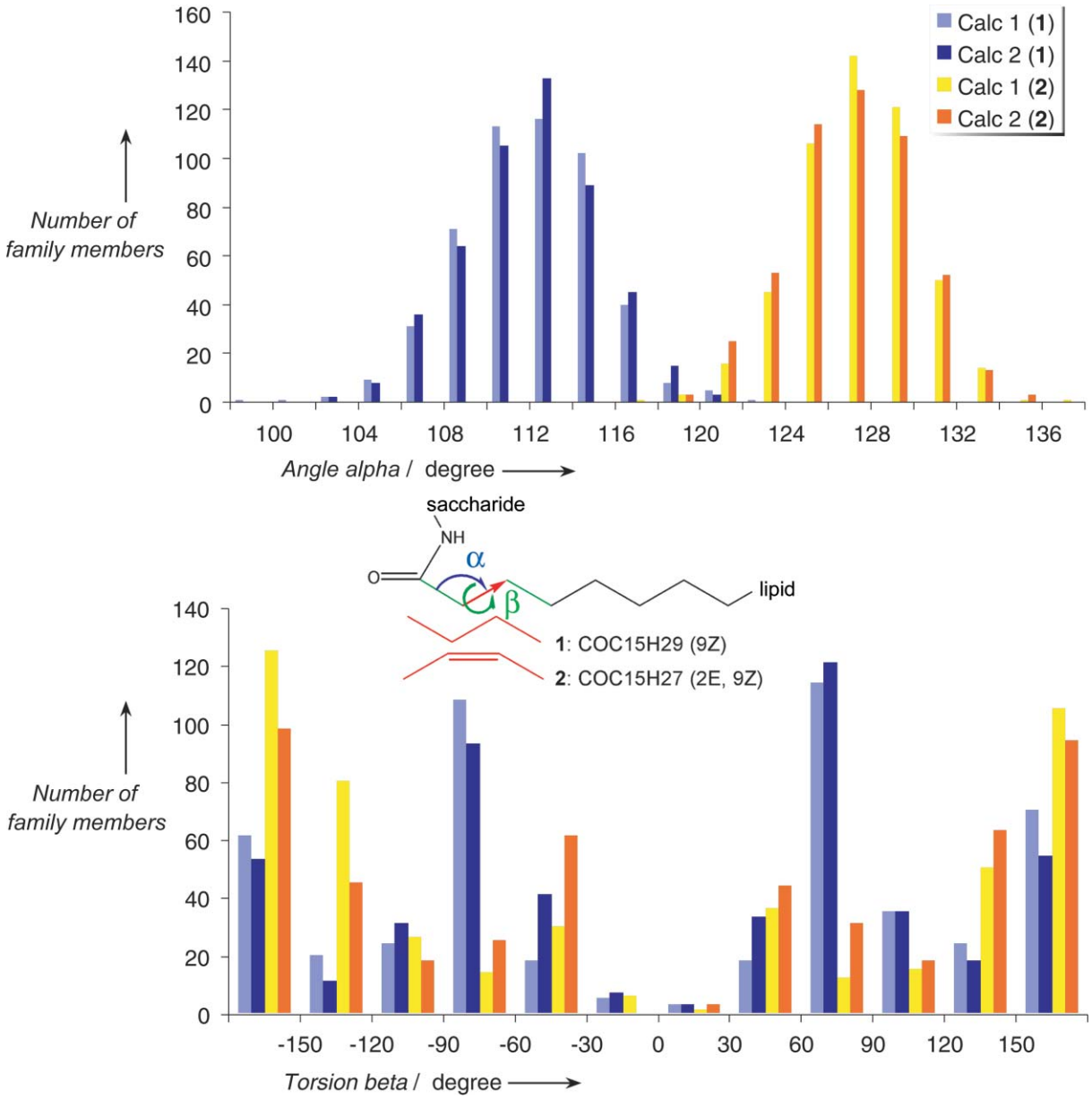

Fig. 3 Plot of the 500 lowest energy conformations classified in families as a function of angle α and torsional angle β (shown in blue or green, respectively, in the inset diagram). Blue colored columns represent the conformations of **1** (two different calculations), yellow and orange the conformations of **2** (two different calculations).

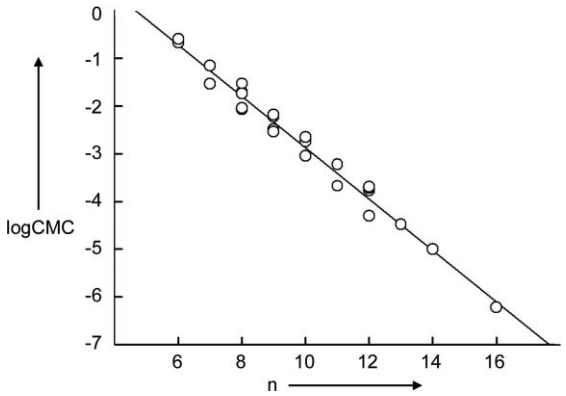

Fig. 4 Plot of log CMC *versus* lipid chain length (n) for carbohydrate containing detergents. Data taken from the Anatrace catalog.[9]

Fig. 4 were obtained from a number of experimental methods.[9] The correlation shown in Fig. 4 predicts that **1** and **2**, which contain C16 lipids, should have CMCs in the low micromolar range. This concentration range is similar to the physiological concentration of LCOs discussed by Geurts and Bisseling.[6]

Diffusion ordered spectroscopy (DOSY) has been used to study the self-aggregation of detergents.[10] Fig. 5A and 5B shows the measured log diffusion coefficient as a function of LCO concentration. Below the CMC, a constant value of diffusion coefficient will be measured. Above the CMC, aggregation causes an effective increase in the average mass of detergent molecules and this is manifested as a downward deflection towards smaller diffusion coefficients. The data obtained for **4** provides a CMC of 21.4 mM, Fig. 5B, consistent with literature values.[9] The diffusion coefficients of **1** and **2** were calibrated with a series of chitooligosaccharides,[11] and the approximate mean sizes of the LCO aggregates are given to the right of Fig. 5B in terms of their aggregation number. The aggregation profiles of **1** and **2** are similar. Thus, contrary to the modeled conformational behavior, the different levels of lipid unsaturation in the LCOs do not seem to affect the obtained aggregation profiles.

Apart from the DOSY data, the aggregation processes of **1** and **2** were also detected by small upfield and downfield chemical shift changes in the ^{1}H NMR spectra. The C9H/C10H

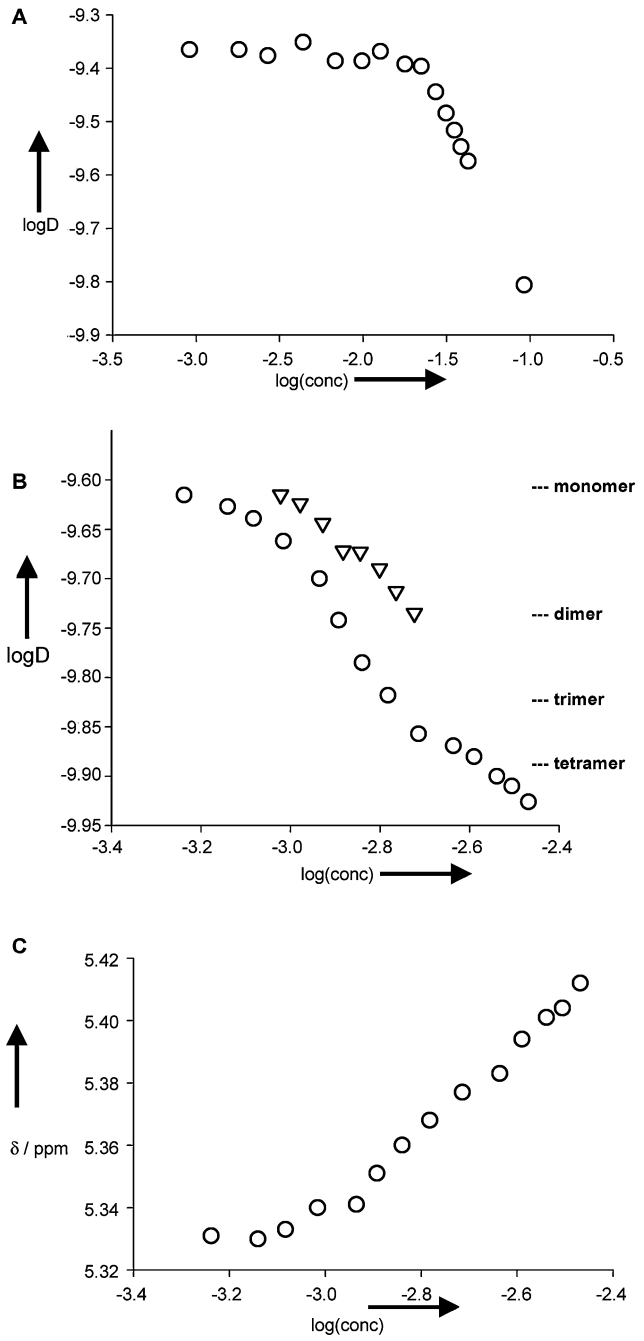

Fig. 5 Double log-plot of experimentally determined diffusion coefficient (*D*) *versus* detergent concentration. A. Data for **4** provide a CMC of 21.4 mM, consistent with literature values.[9] B. Similar data for **1** (circles) and **2** (triangles). The average aggregate size is given to the right of the panel as based on a chitooligosaccharide calibration.[11] C. Concentration-dependent changes in the chemical shifts of the C9H/C10H resonance of **1** is consistent with the diffusion data.

lipid resonances of **1** (0.08 ppm) and the C2H resonance of **2** (0.04 ppm) were most strongly affected by oligomerization. The observed changes in chemical shift were concentration dependent and for **1** they are large enough to be clearly consistent with the changes in log *D*, Fig. 5C.

The lipid moieties of detergents tend to be connected to the C1 position (of the reducing end) of the carbohydrate head group, as in **4**, with any saccharide extension tending to occur at the C4 position. In contrast, the lipid moieties of LCOs are attached to the C2 of the non-reducing end with the oligosaccharide extension proceeding from the adjacent C1 position. Therefore, the oligosaccharide moieties of **1** and **2** are likely to provide a larger steric hindrance to micelle formation, as suggested in Fig. 5, than the carbohydrate moieties of detergents related to **4**, with similar length C16 lipid chains (and CMCs of around 1 μM). The high measured CMCs of **1** and **2**, about 1000-fold greater than those expected from Fig. 4, apparently reflect this steric hindrance. Thus, according to these data, pure, LCO aggregates are unlikely to be formed under the physiological, micromolar levels of LCOs (Fig. 5). LCOs carrying C18 or C20 lipid chains have predicted CMCs in the submicromolar range according to Fig. 4, but the values, when corrected by three orders of magnitude, are still likely to be in excess of 10 μM. Nevertheless, we cannot preclude the possibility that LCOs form mixed micelles with natural lipids or enter a membrane-bound state[5] on the basis of our data. Overall, our data suggest that LCOs probably display a monomeric distribution under physiological conditions.

Experimental confirmation of modeling data by NOESY

A previous study of **1** in aqueous and DMSO solution was carried out at 2.5 mM concentration.[7] Molecular modeling suggested contacts between the lipid and oligosaccharide moieties in aqueous solution that would be absent in DMSO. NOESY, which reports contacts of less than 5 Å, confirmed the contacts between the lipid and carbohydrate moieties. However, NOESY cannot distinguish between intra- and inter-molecular contacts in aggregated forms of LCOs. In fact, the results of the DOSY experiments gathered in Fig. 5, indicate that the original NOESY studies were carried out on an aggregated form of **1**.[7] Therefore, it is important to confirm the structures of **1** and **2** under monomeric conditions.

The NMR assignments of **1** and **2** were confirmed with NOESY and TOCSY experiments.[7,12] The ~1 mM concentrations of monomeric **1** and **2** were sufficient to obtain a significant number of assignments. Severe overlap within the carbohydrate ring proton region and lipid proton region precluded a complete, unambiguous assignment. However, fortunately there is a clear distinction between signals arising within the carbohydrate scaffold (3.0–4.7 ppm) and within the lipid moiety (0.8–1.5 and 2.15–2.3 ppm). Comparison of 2D NMR spectra obtained at monomeric and aggregated concentrations revealed changes in peak patterns, most notably for long mixing time NOESY spectra of **2**.

Fig. 6 provides partial NOESY spectra for **1** and **2** at monomeric and aggregated concentrations. NOEs indicating contacts between lipid and tetrasaccharide moieties are boxed. These NOEs carry important information about the relative orientation of the lipid and tetrasaccharide moieties as they typically indicate distances of less than 5 Å.[13] The NOEs obtained under aggregated concentrations (Fig. 6B, 6D) are ambiguous as they may originate from intra- or inter-molecular contacts. Also, the size of the molecular aggregate (aggregates of **1** are twice the size of aggregates of **2**, according to Fig. 5B), affects NOE intensity. The NOEs obtained under monomeric concentrations (Fig. 6A, 6C) are of more value in confirming the molecular modeling data as they arise only from intramolecular contacts. Lipid-tetrasaccharide NOEs are observed in the monomeric form of **1** (Fig. 6A) but not in the monomeric state of **2** (Fig. 6C). These experimental data unambiguously indicate that the additional double bond in **2** indeed provides a different relative orientation of the lipid and tetrasaccharide than in **1**, and that the lipid chain partially docks with the tetrasaccharide moiety in **1**, as suggested by the modeling protocol.

Moreover, in order to assess that the lack of lipid–sugar cross peaks in the NOESY spectra of monomeric **2** does not arise from a particular molecular size or motional behavior (that could give zero NOEs even for proton pairs close in space, for $\omega\tau_c$ *ca.* 1.1), ROESY experiments were also performed. It is well known that ROE cross peaks are always positive, independent of the size and motions of the molecule of interest. ROE crosspeaks between lipid and carbohydrate protons were observed in spectra of monomeric **1**, but were absent for monomeric **2**.

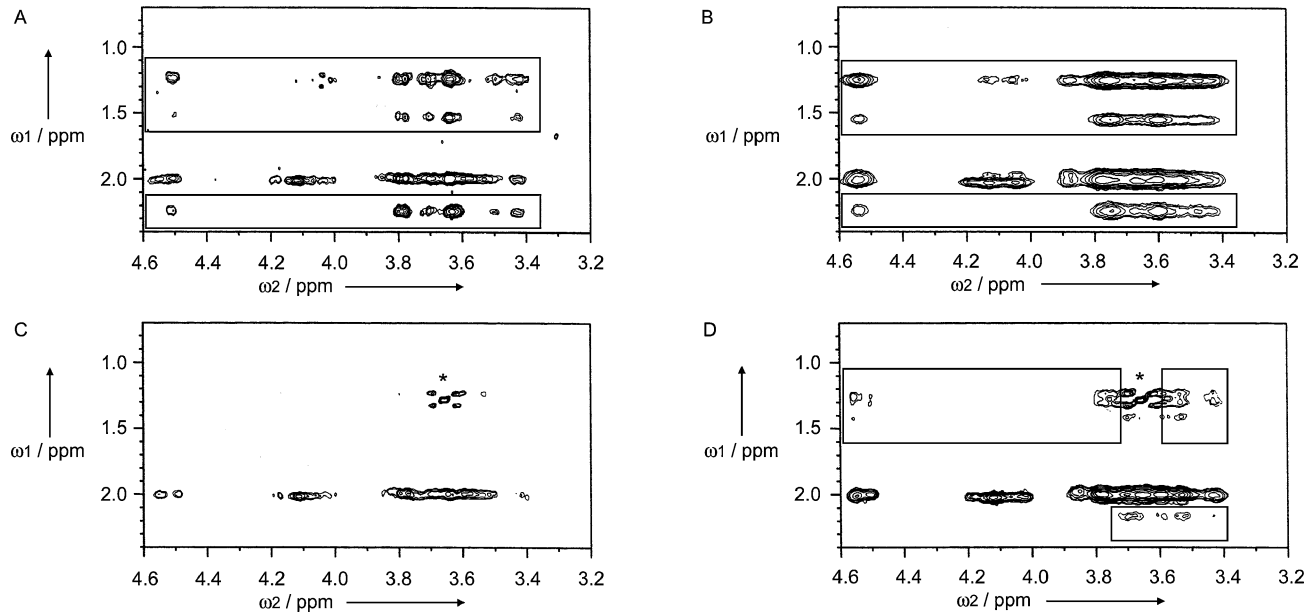

Fig. 6 Lipid-tetrasaccharide contacts at different concentrations and aggregated states of **1** and **2**. A. 1.1 mM, monomeric **1**. B. 2.5 mM, aggregated **1**. C. 1.0 mM monomeric **2**. D. 1.9 mM aggregated **2**. Unambiguous lipid-tetrasaccharide NOEs are shown in the boxes. Other NOEs represent zero-quantum peaks or potential lipid-tetrasaccharide NOEs (unboxed) overlapped with NOEs between the three overlapping N-acetyl groups and neighboring protons in the tetrasaccharide moiety. All NOESY spectra were collected with 300 ms mixing times.

The role of spin diffusion in the transfer of magnetization throughout the lipid chain, the saccharide scaffold and between them was also analyzed. For example, spin diffusion can involve the transfer of NOE magnetization between several proton pairs within the lipid chain. Indeed, some spin diffusion was observed in the 300 ms mixing time NOESY along the lipid chain. Many of the lipid-carbohydrate NOEs observed for **1** in Fig. 6A were still observed in 75 ms NOESY experiments, where spin diffusion is insignificant for a molecule of this size at 500 MHz. This suggests that the lipid–carbohydrate NOEs of monomeric **1** are therefore direct and not the product of spin diffusion.

Therefore, proton pairs of the lipid and carbohydrate moieties of monomeric **1** are less than 5 Å apart for a sufficient proportion of time to produce significant NOE/ROE peaks. In contrast, no similar lipid–carbohydrate cross peaks are observable for **2**, using two different NMR experiments and a range of mixing times. Thus, it can be safely assumed that the NOESY data support the molecular modeling results and that average relative orientation of the lipid chain *versus* the tetrasaccharide scaffold significantly differ between **1** and **2**.

Effect of LCOs structure on their affinity for Nod factor binding sites

LCO-binding proteins, the so-called Nod factor binding sites (NFBS), have been characterized from different legumes.[14,15] Binding studies have shown that binding sites characterized in cell suspension cultures of *Medicago varia* and *Phaseolus vulgaris* exhibit different selectivity towards the structural motifs of the LCOs produced by their respective symbionts. The different receptors appear to show specificity for small structural features such as a LCO sulfate group or double bond. Therefore, it was proposed that the differences in LCO selectivity by receptors was a result of receptor evolution and that each receptor had specific cavities for LCO pendant groups.[15] As strong binding is best achieved by a receptor binding to the lowest energy conformation of the ligand, there is a benefit to those bacteria that produce LCOs that have the correct shape for the plant receptors. This idea seems to be supported by a recent study on the possible binding of **2** to the lectin-like moiety of *M. truncatula* receptor kinases.[16] Although we should consider that Nod factors have not yet been shown to directly interact with this moiety, it is worth noting that the α (125°) and β (167°) angles of bound **2** in the published structure of the complex[16] agree well with those found for the free form of **2** in this study.

We have shown herein that two closely related LCOs indeed have distinct low energy conformations. This leads us to conclude that the shape requirement of LCO-binding proteins can include both specific binding pockets for pendant groups and also the influence of the pendant groups on the overall three dimensional shape of the molecule in its unbound state.

Conclusions

The obtained conformational families of **1** and **2** have distinct lipid orientations relative to their common tetrasaccharide scaffold. These conformations would appear to support the idea that the lipid moieties of LCOs lend a degree of ligand specificity to Nod factor receptors. The use of the lipid moiety in a membrane-anchoring role does not appear to be supported as Nod factors appear to interact first with the plant cell-wall.[4] Pure, aggregated forms of LCOs appear to be physiologically unlikely to occur as the measured CMCs for **1** and **2** are about 1000-fold higher than their physiological concentrations. The combination of DOSY and NOESY data illustrates the importance of supporting modeling studies of LCOs with experimental data collected under monomeric conditions in order to discriminate between intra- and inter-molecular interactions. These studies also indicate that small differences in LCO functionality can have a strong influence on three-dimensional shape. In turn, this can contribute to the specificity of LCO receptors in legume root cells for LCOs adopting the correct conformation.

The recent identification of genes involved in Nod factor perception is an important step forward to decipher the molecular basis of Nod factor recognition.[17,18] This will help to evaluate the binding properties of the encoded proteins (receptor like kinases with an extracellular domain containing LysM motifs, known to interact with glycans) and also to clarify the roles of the previously characterized Nod factor binding sites.

Experimental

General

The synthesis and NMR assignment of LCO **1** has been described by Gonzalez *et al.* and Rasmussen *et al.*[7,12] LCO **2**

is described by Rasmussen *et al.*[12] β-D-octyl glucopyranoside (**4**) was purchased from Sigma.

Molecular modeling

The conformational behavior of LCOs **1** and **2** were studied with the use of a simulated annealing process. All calculations, manipulations and the conformational analysis of molecules were performed on Silicon Graphics workstations using the molecular modeling package SYBYL (Tripos, St Louis) together with the TRIPOS force-field[19] with incorporation of energy parameters developed for carbohydrate.[20] In a first step the initial molecules **1** and **2** were constructed according to previous modeling study[7] and atomic charges derived with the use of the MNDO program.[21] The simulated annealing protocol began with an energy minimization of the two starting structures. Every model was then submitted to 500 individual runs in which the system was heated to a temperature of 500 K and maintained at this temperature for 500 fs. Afterwards the system was cooled down to a minimum temperature of 50 K in 500 fs. This resulted in a total simulation time of 1000 fs per cycle. The dielectric constant used in this experiment was $\varepsilon = 80.0$. To avoid the formation of a distorted geometry of the pyranose ring at high temperature, two torsional restraints were introduced per ring (C1–C2–C3–C4, C4–C5–O5–C1, force constants of 3 kcal mol^{-1} $Å^{-2}$), giving a total of 8 restraints for the tetrasaccharide part of each LCO. Using this simulated annealing protocol, a set of 15000 conformations (30 per run) per LCO was obtained. The 500 final conformations of each run with the lowest energy were selected and subjected to a geometrical analysis using the SYBYL programming language (SPL) together with the molecular spreadsheet. The geometrical classification included calculation of distances, angles and torsions between atoms, but also between sugar and lipid planes and centroid of rings. All data are evaluated with respect to the minimum, maximum and mean value of each distance, angle and torsion within the group of 500 conformations. Furthermore the conformations have been classified into families by subdividing the whole range of each distance or angle in smaller sections. A graphical interpretation of the results has been done using EXCEL. To compare directly the different families of conformations of **1** and **2** the 50 conformations with lower energy have been superposed by fitting on the three connecting glycosidic oxygen of the tetrasaccharide.

Diffusion ordered spectroscopy

All samples were prepared in 20 mM phosphate buffer, 100 mM NaCl, pH 5.6, 100% D_2O. The standard BRUKER DOSY protocol was used at 298 K on an AVANCE 500 MHz equipped with a broad-band z-gradient probe.[22] Thirty-two 1D ^1H spectra were collected with a gradient duration of $\delta = 2$ ms and an echo delay of $\Delta = 100$ ms. Acquisition times of 8–15 min (8–16 scans) were required for the samples. Samples of *N*-acetyl glucosamine oligomers, $(GlcNAc)_n$ with $n = 1$–6 were used to calibrate the micelle size ($\log D = -0.427 \log MW - 8.231$, $r^2 = 0.983$), as described in Groves *et al.*[11] The ledbpg2s pulse sequence, with stimulated echo, longitudinal eddy current compensation, bipolar gradient pulses and two spoil gradients, was run with a linear gradient (53.5 G cm^{-1}) stepped between 2% and 95%. The 1D ^1H spectra were processed and automatically baseline corrected. The diffusion dimension, zero-filled to 1 k, was exponentially fitted according to preset windows for the diffusion dimension ($-8.5 < \log D < -10.0$).

NMR spectroscopy

The noesyphpr pulse sequence was used to collect NOESY data on **1** and **2**. The dipsi2phpr and roesyphpr.2 pulse sequences were used to collect coupling data (TOCSY) and NOE data in the rotating frame (ROESY) for **1** and **2**. Spectra were collected with mixing times between 20 and 300 ms on a Bruker AVANCE 500 MHz spectrometer at 298 K. The concentrations of **1** and **2** are as given in the legend to Fig. 6.

Acknowledgements

We thank the EU for financial support through the SACC-SIGNET project (HPRN-CT-2002-00251). The Madrid team also acknowledges Dirección General de Investigación of Spain, Grant BQU2003-03550-C03-01 for funding.

References

1 G. D. May and R. A. Dixon, *Curr. Biol.*, 2004, **14**, R180–R181.
2 J. V. Cullimore, R. Ranjeva and J. J. Bono, *Trends Plant Sci.*, 2001, **6**, 24–30.
3 W. D'Haeze and M. Holsters, *Glycobiology*, 2002, **12**, 79R–105R.
4 J. Goedhart, J. J. Bono, T. Bisseling and T. W. Gadella Jr., *Mol. Plant-Microbe Interact.*, 2003, **16**, 884–892.
5 J. Goedhart, H. Rohrig, M. A. Hink, A. Van Hoek, A. J. Visser, T. Bisseling and T. W. Gadella Jr., *Biochemistry*, 1999, **38**, 10898–10907.
6 R. Geurts and T. Bisseling, *Plant Cell*, 2002, **14**, S239–S249.
7 L. Gonzalez, M. Bernabe, J. F. Espinosa, P. Tejero-Mateo, A. Gil-Serrano, N. Mantegazza, A. Imberty, H. Driguez and J. Jimenez-Barbero, *Carbohydr. Res.*, 1999, **318**, 10–19.
8 M. Schultze, B. Quiclet-Sire, E. Kondorosi, H. Virelizer, J. N. Glushka, G. Endre, S. D. Gero and A. Kondorosi, *Proc. Natl. Acad. Sci. U. S. A.*, 1992, **89**, 192–196.
9 *Anatrace catalog*, 2004, pp 111–113.
10 U. R. K. Kjellin, J. Reimer and P. Hansson, *J. Colloid Interface Sci.*, 2003, **262**, 506–515.
11 P. Groves, M. O. Rasmussen, M. D. Molero, E. Samain, F. J. Cañada, H. Driguez and J. Jiménez-Barbero, *Glycobiology*, 2004, **14**, 451–456.
12 M. O. Rasmussen, B. Hogg, J. J. Bono, E. Samain and H. Driguez, *Org. Biomol. Chem.*, 2004, **2**, 1908–1910.
13 J. Cavanagh, W. J. Fairbrother, A. G. Palmer and N. J. Skelton, in *Protein NMR spectroscopy: principles and practice*. Academic Press, San Diego, USA, 1993, p. 384–402.
14 F. Gressent, S. Drouillard, N. Mantegazza, E. Samain, R. A. Geremia, H. Canut, A. Niebel, H. Driguez, R. Ranjeva, J. Cullimore and J. J. Bono, *Proc. Natl. Acad. Sci. U. S. A.*, 1999, **96**, 4704–4709.
15 F. Gressent, N. Mantegazza, J. V. Cullimore, H. Driguez, R. Ranjeva and J. J. Bono, *Mol. Plant-Microbe Interact.*, 2002, **15**, 834–839.
16 M. T. Navarro-Gochicoa, S. Camut, A. C. Timmers, A. Niebel, C. Herve, E. Boutet, J. J. Bono, A. Imberty and J. V. Cullimore, *Plant Physiol.*, 2003, **133**, 1893–1910.
17 E. Limpens, C. Franken, P. Smit, J. Willemse, T. Bisseling and R. Geurts, *Science*, 2003, **302**, 630–633.
18 S. Radutoiu, L. H. Madsen, E. B. Madsen, H. H. Felle, Y. Umehara, M. Grønlund, S. Sato, Y. Nakamura, S. Tabata, N. Sandal and J. Stougaard, *Nature*, 2003, **425**, 585–592.
19 M. Clark, R. D. Cramer and N. Vanopdenbosch, *J. Comput. Chem.*, 1989, **10**, 982–1012.
20 A. Imberty, C. Monier, E. Bettler, S. Morera, P. Freemont, M. Sippl, H. Flockner, W. Ruger and C. Breton, *Glycobiology*, 1999, **9**, 713–722.
21 M. J. S. Dewar and W. Thiel, *J. Am. Chem. Soc.*, 1977, **99**, 4907–4917.
22 R. Kerssebaum, in *DOSY and Diffusion by NMR*, Bruker BioSpin, Rheinstetten, Germany, 2002.